

Article

Formation, Stability, and Crystallinity of Various Tricalcium Aluminate Polymorphs

Simona Ravaszová ¹, Karel Dvořák ^{1,*} , Martin Boháč ², Dalibor Všianský ³ and Andrea Jančíková ¹

¹ Faculty of Civil Engineering, Brno University of Technology, Veveří 331/95, 602 00 Brno, Czech Republic; ravaszova.s@fce.vutbr.cz (S.R.); janciku.a@fce.vutbr.cz (A.J.)

² Research Institute for Building Materials, Hněvkovského 30/65, 617 00 Brno, Czech Republic; bohac@vush.cz

³ Department of Geological Sciences, Faculty of Science, Masaryk University, Kotlářská 267/2, 611 37 Brno, Czech Republic; dalibor@sci.muni.cz

* Correspondence: dvorak.k@fce.vutbr.cz; Tel.: +420-775906555

Abstract: Tricalcium aluminate is an important phase of Portland clinker. In this paper, three polymorphs of C₃A were prepared by means of the solid-state synthesis method using intensive milling of the raw material mixture which was doped with various amounts of Na₂O and sintered at a temperature of 1300 °C for 2 h. The final products were evaluated through X-ray diffraction using Rietveld analysis. The effect of the Na dopant content on the change in the crystalline structure of tricalcium aluminate was studied. It was proven that the given preparation procedure, which differed from other studies, was close to the real conditions of the formation of Portland clinker, and it was possible to prepare a mixture of different polymorphs of calcium aluminate. Fundamental changes in the crystal structure occurred in the range of 3–4% Na, when the cubic structure changes to orthorhombic. At a dosage of Na dopant above 4%, the orthorhombic structure changes to a monoclinic structure. There are no clearly defined boundaries for the existence of individual C₃A phases; these phases arise at the same time and overlap each other in the areas of their formation at different Na doses.

Keywords: tricalcium aluminate; polymorphism; cubic; orthorhombic; monoclinic; crystallite size



Citation: Ravaszová, S.; Dvořák, K.; Boháč, M.; Všianský, D.; Jančíková, A. Formation, Stability, and Crystallinity of Various Tricalcium Aluminate Polymorphs. *Materials* **2024**, *17*, 735. <https://doi.org/10.3390/ma17030735>

Academic Editors: Milena Pavlíková, Peiyu Yan, Yao Luan and Chunsheng Zhou

Received: 29 November 2023

Revised: 12 January 2024

Accepted: 31 January 2024

Published: 3 February 2024



Copyright: © 2024 by the authors. Licensee MDPI, Basel, Switzerland. This article is an open access article distributed under the terms and conditions of the Creative Commons Attribution (CC BY) license (<https://creativecommons.org/licenses/by/4.0/>).

1. Introduction

Due to economic and environmental pressures, especially regarding the production of a lower volume of CO₂, modern cement materials are increasingly complex from a chemical and mineralogical point of view [1]. The use of alternative fuels such as waste materials, biomass, and municipal solid waste can reduce our dependence on fossil fuels, reduce greenhouse gas emissions, and improve energy efficiency. However, this represents not only economic advantages but also technological challenges. This trend inevitably leads to a change in the properties of the individual phases of Portland cement. The properties of these components can therefore differ significantly from those expected for traditional Portland cement in previous years. This requires extensive research and testing [2–6].

Tricalcium aluminate (C₃A) is one of the most important components of Portland cement (OPC). Tricalcium aluminate with a melting point of 1540 °C belongs to the group of the most represented calcium–aluminate phases in clinker, forming approximately 7 to 15 wt.% of it [7,8]. Currently, the formation of tricalcium aluminate during sintering is often affected by various foreign ions. These ions change the resulting structure of tricalcium aluminate and thus also the course of hydration of the cement phase. The most common C₃A modifiers are sodium and potassium ions in the form of alkalis [9]. They tend to be contained in larger or smaller quantities in raw materials to produce clinker. Their content is measured and controlled, which enables additional correction. In contrast, monitoring the quantitative representation of ions introduced into the material due to the burning of solid alternative fuels is relatively difficult to implement. Nowadays, cement plants use a

whole range of secondary fuels for firing clinker in the production of cement. The most commonly used secondary raw materials in incineration are waste oil, used tires, meat, and bone meal or sorted waste, which includes mixed plastics, textiles, textile fibers, carpets, rubber, paper, plastic–paper composite packaging, and chipboard [7–10].

The most important property of C_3A affects the processability of cement paste [11,12].

C_3A occurs in clinker in three modifications depending on the content of alkalis, especially sodium ions. Other oxides that cause C_3A modification are K_2O , SiO_2 , MgO , and Fe_2O_3 [7,8,13,14]. Pure tricalcium aluminate occurs in a cubic structure. Modification with Na_2O in particular changes the cubic structure to an orthorhombic structure, monoclinic structure, and two metastable structures, i.e., tetragonal (high-temperature polymorph) and a weakly crystalline form, the so-called “proto- C_3A ”. The reactivity of the given structures is different and so is their course of hydration [15–17].

One calcium ion is replaced by two sodium ions. One sodium ion takes the place of the original Ca^{2+} and the other is in the center of the $(Al_6O_{18})^{18-}$ ring. The general formula of C_3A modified by sodium ions can be written as $Na_{2x}Ca_{3-x}Al_2O_6$ where x denotes the amount of calcium ions substituted by sodium ions. As x increases from 0 to 0.25, the crystal system changes from cubic to orthorhombic and then to monoclinic at room temperature. In the C_3A crystal structure, there are eight sites on the triaxial axes where additional atoms can be inserted. The size of Ca^{2+} and Na^+ ions is similar, and it is therefore possible to state that Na^+ ions replace Ca^{2+} atoms in their places in the structure [18,19]. Sodium (Na), which replaces calcium (Ca) in the crystal lattice, occupies a space that is about the same size but slightly larger. When calcium is substituted for sodium, the gaps between the atoms are not filled, leading to a gradual change in the crystal structure. As a result, the initially symmetric cubic lattice becomes a less symmetric orthorhombic or monoclinic [20,21].

Tricalcium aluminate is formed by a solid–solid reaction between CaO and Al_2O_3 indirectly through the phases, with various ratios between CaO and Al_2O_3 . Despite long-term application, there is still no consensus regarding the kinetic and mechanistic aspects of its formation [22–24].

The preparation of high-purity C_3A single phases differs considerably from industrial production. In addition to the classic method based on a high-temperature reaction in the solid phase, there are also alternative methods such as the sol–gel method, combustion syntheses, or synthesis using mechanochemical activation.

The literature [25] states that mechanochemical activation can significantly affect the rate of reactions, whereby the most reproducible and consistent results were obtained under conditions of good interparticle contact with controlled pretreatment to define the physical structure. Mechanochemical activation supports the course of reactions in the solid phase, as it increases the specific surface area and local thermal effects. This is a very energy-intensive preparation, in which the individual processes occur at lower temperatures, however, which, on the other hand, makes it possible to reduce the overall temperature and firing time. The course of the reaction is similar to the high-temperature method [26,27].

Finding a suitable procedure for the sol–gel synthesis of calcium–aluminate phases turned out to be somewhat problematic. For the preparation of calcium–aluminate phases, the Pechini method and its modified versions, which also belong to the group of sol–gel methods, have proven themselves. However, these methods are very far from the real conditions for the formation of calcium aluminate phases in Portland clinker [28].

Therefore, this article is devoted to the traditional method of reaction in the solid phase, which represents the oldest method used for the preparation of the calcium–aluminate phase, but it is still the most frequently used nowadays. In this method, thorough homogenization of the raw materials is very important. If the starting mixture is not homogeneous, the product tends to be contaminated with unreacted starting substances. Preparing a pure phase of the desired composition is often problematic with this method. Unwanted phases are often present in the product. They are present in the product if the reaction does not take place completely or if there are inhomogeneities in the reaction mixture. In the area

of inhomogeneities, local phase equilibrium is established, and the corresponding phase is formed.

Previous studies [9,15,16,19–21,29–31] on calcium–aluminate phases often use a different methodology than the one used in this study. This article is devoted to the preparation of various C_3A polymorphs when the raw material mixture is doped with sodium, which is added to the raw material mixture before sintering. The aim is to study the formation of individual polymorphs that are formed in parallel. In this way, the preparation procedure presented in this study is close to the real conditions of Portland clinker production. The goal is to prepare pure phases through solid-state synthesis in the highest possible purity.

This article deals with the preparation of various polymorphs of tricalcium aluminate by means of the solid-state method. The aim is to use a simple preparation method that includes mechanical activation of the raw material mixture doped with different Na content and one-step firing to prepare tricalcium aluminate at the highest possible purity.

To evaluate the purity of the prepared C_3A samples, the Rietveld method was chosen, which involved the Sherrer equation to monitor the crystallinity of the prepared tricalcium aluminates.

2. Materials and Methods

2.1. Raw Material Mixture Composition

Calcium carbonate ($CaCO_3$, p.a. purity, Penta, Praha, Czech Republic), aluminum oxide (Al_2O_3 , p.a. purity, Penta, Praha, Czech Republic), and sodium carbonate (Na_2CO_3 , p.a. purity, Penta, Praha, Czech Republic) were used as precursors for the synthesis of tricalcium aluminate. The composition of the raw material mixture for the preparation of tricalcium aluminate was based on already published data [9,30]. The $CaCO_3$ and Al_2O_3 were mixed in a stoichiometric ratio of 3 mol CaO and 1 mol Al_2O_3 , which corresponds to the cubic C_3A modification. Stabilization with sodium (added in the form of sodium carbonate) is necessary to obtain the orthorhombic and monoclinic forms. The content of Na_2O added to the raw material mixture for the formation of orthorhombic and monoclinic C_3A is shown in Table 1.

Table 1. Composition of Na-substituted C_3A raw material mixture.

Label	$CaCO_3$ [g]	Al_2O_3 [g]	Na_2CO_3 [g]	Total
0.0% Na_2O	22.40	7.60	0.00	30.000
0.5% Na_2O	22.40	7.60	0.26	30.260
1.0% Na_2O	22.40	7.60	0.51	30.510
1.5% Na_2O	22.40	7.60	0.77	30.770
2.0% Na_2O	22.40	7.60	1.03	31.030
2.5% Na_2O	22.40	7.60	1.28	31.280
3.0% Na_2O	22.40	7.60	1.54	31.540
3.5% Na_2O	22.40	7.60	1.8	31.800
4.0% Na_2O	22.40	7.60	2.05	32.050
4.5% Na_2O	22.40	7.60	2.31	32.310
5.0% Na_2O	22.40	7.60	2.57	32.570
5.5% Na_2O	22.40	7.60	2.82	32.820
6.0% Na_2O	22.395	7.605	3.08	33.080

In order to ensure a sufficient amount of Na, which suffers from the relatively high volatility of sodium at high temperatures and resulting losses during sintering, Na_2CO_3 was added to the calculated stoichiometric ratio of CaO and Al_2O_3 .

2.2. Tricalcium Aluminate Preparation

Milling and homogenization of the raw material mixture were carried out through high-energy wet milling in a planetary mono mill (Pulverisette 6, Fritsch, Idar-Oberstein, Germany). A 40 mL steel capsule and 25 steel balls with a diameter of 20 mm were used. The basic ratio of dry ingredients and water was 30 g of the raw material mixture and 30 g

of water. The water/powder ratio of 1.0 was used. The milling mode of 350 rpm for 15 min was selected. A Malvern Mastersizer 2000 laser granulometer (Malvern Panalytical Ltd., Malvern, UK) with a hydro 2000 G fluid dispersion unit, using 2-2-isopropanol as the dispersing agent was used for determining the granulometry. After wet milling, all samples were dried in a laboratory oven (Binder C170, Binder GmbH., Tuttlingen, Germany) at a temperature of 105 °C for 24 h. The slurry spontaneously formed solid nodules during the drying process, which were subsequently placed in 30 mL platinum crucibles. The sintering process was carried out in a high-temperature furnace (2017 S, Clasic CZ s.r.o., Řevnice, Czech Republic). The firing mode was designed so that the carbonates first decompose at a temperature of 1000 °C for 1 h and then, the synthesis itself takes place in the solid phase at a temperature of 1300 °C for 2 h. The heating rate was 8 °C/min. At the end of the firing mode, the crucibles were removed from the furnace and immediately cooled by a stream of cold air to room temperature. The sintered products were subjected to milling in a vibratory disc mill (RS 200, Retsch, Haan, Germany) at 1000 rpm for 20 s. After that, 5 g of sintered products in the form of powder was milled to the required fineness for X-ray analysis in a mill (McCrone Micronising Mill, Glen Creston, London, UK) for 150 s in 15 mL of isopropanol.

2.3. X-ray Diffraction Analysis

The XRD analysis was performed using a multifunctional diffractometer (XRD, Empyrean, PANalytical B.V., Almelo, The Netherlands). The Θ - Θ reflection Bragg–Brentano para focusing geometry device is equipped with a Cu anode ($\lambda = 1.54184 \text{ \AA}$), programmable divergence slits, and a PIXcel3D detector (Empyrean, PANalytical B.V., Almelo, The Netherlands) with 255 active channels, with an accelerating voltage of 45 kV, a beam current of 40 mA, and a diffraction angle of 2Θ in the range from 5 to 60° with a step size of 0.013° and 38 s per step. The total time per scan was 12 min. Each sample was measured four times, and the scans were next simply summed. The polymorphic purity of the samples was verified via XRD using the Rietveld method. The ICSD database (released in 2012) was used to qualitatively analyze the diffraction patterns. HighScore plus software (3.0e, PANalytical B.V., Almelo, The Netherlands) was used to identify the individual phases, perform their quantification, and determine the amount of the amorphous phase.

2.4. Tricalcium Aluminate Crystallinity

The size of the crystallites was evaluated on a selected diffraction line with the major crystallographic direction. Calculation of the crystallite size is based on the measurement of full width at half maximum (FWHM) via the Scherrer equation [32] with Warren correction [33]; see Equation (1):

$$L = \frac{K \cdot \lambda}{\cos \theta} \cdot \frac{1}{\beta} = \frac{K \cdot \lambda}{\cos \beta} \cdot \frac{1}{\sqrt{B^2 - b^2}} \quad (1)$$

L is the crystallite size, K is the Scherrer constant (the value of 0.89 was used), $\lambda = K_{\alpha 1}$ is the wavelength of X-ray radiation, θ is the diffraction angle, B is the FWHM, and b is the FWHM of the size/strain standard used (lanthanum hexaboride).

The instrument broadening was defined using the LaB_6 standard. LaB_6 peaks were determined in the positions identical to the selected diffraction lines using HighScore plus software, see Figure 1. The FWHM values of LaB_6 were calculated from Equation (1) [34].

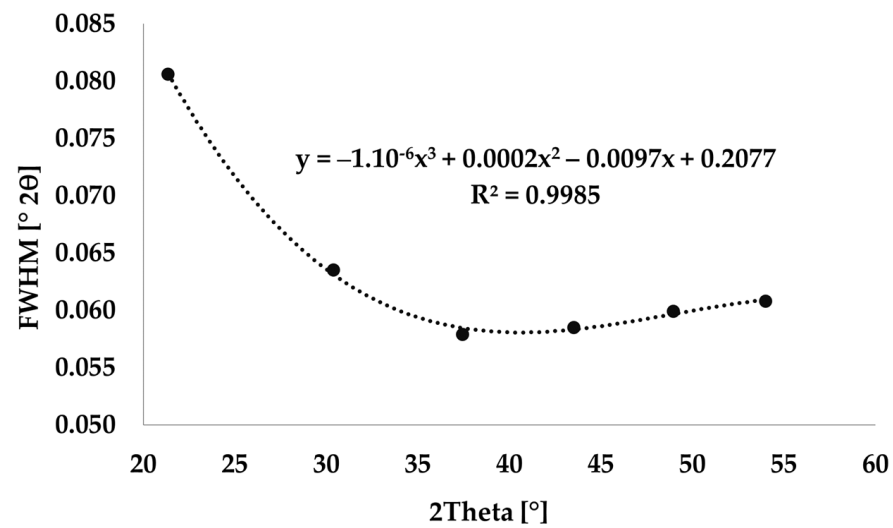


Figure 1. Instrumental broadening measured using LaB₆.

3. Results and Discussion

3.1. Tricalcium Aluminate Preparation

The distribution of particles after the homogenization of raw materials through high-energy milling was determined using laser granulometry; see Figure 2.

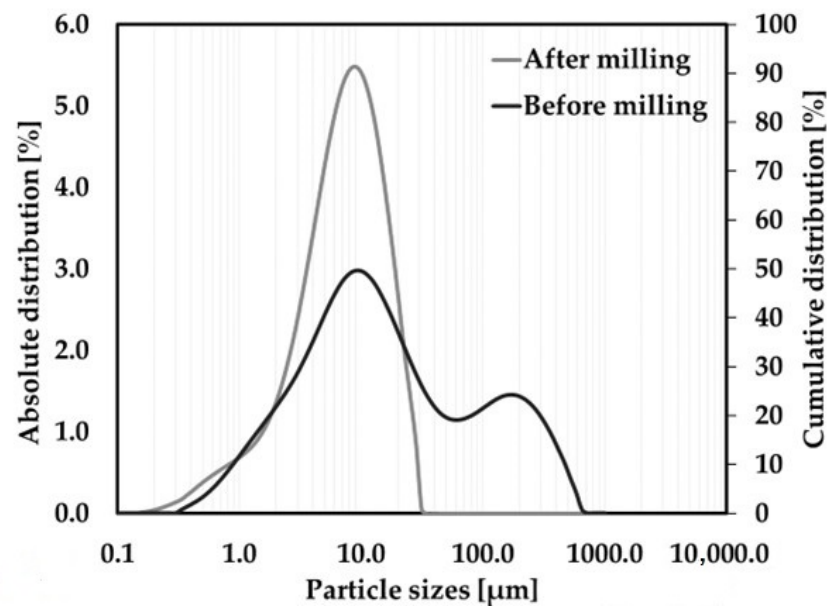


Figure 2. Particle distribution (PSD) of the raw material mixture.

The median particle size of the raw material mixture before homogenization in the Pulverisette 6 laboratory mill (Pulverisette 6, Fritsch, Idar-Oberstein, Germany) was 12.3 μm. After 15 min of milling at 350 rpm, the raw material mixture was refined with a median particle size of 6.8 μm.

3.2. X-ray Diffraction Analysis

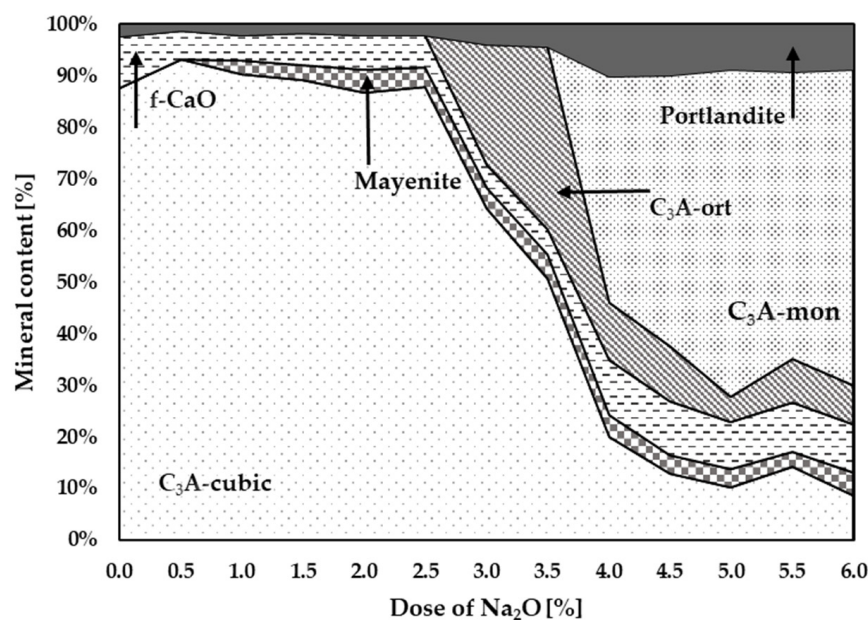
Table 2 shows the quantitative mineral composition of each sample. The results of the Rietveld analysis are presented in Appendix A.

Table 2. Rietveld refinement quantified phase composition of the samples.

Na ₂ O [%]	C ₃ A-c	C ₃ A-o	C ₃ A-m	Mayenite	f-CaO	Portlandite	Total	GOF
0.0	89.7	0.0	0.0	0.0	8.0	2.3	100.0	2.55
0.5	94.4	0.0	0.0	0.0	4.5	1.2	100.1	2.48
1.0	92.1	0.0	0.0	2.7	3.2	2.0	100.0	2.54
1.5	90.5	0.0	0.0	3.1	4.7	1.6	99.9	2.49
2.0	88.8	0.0	0.0	4.4	4.6	2.2	100.0	2.59
2.5	89.9	0.0	0.0	4.0	4.0	2.2	100.1	2.60
3.0	66.9	24.3	0.0	4.0	0.8	4.0	100.0	2.30
3.5	52.9	36.8	0.0	5.0	0.6	4.6	99.9	2.48
4.0	22.2	12.2	48.9	4.8	0.6	11.3	100.0	1.69
4.5	14.3	12.0	58.3	3.8	0.7	10.9	100.0	1.68
5.0	11.0	5.6	69.5	4.0	0.4	9.5	100.0	2.27
5.5	15.7	9.2	61.3	3.0	0.5	10.2	99.9	2.19
6.0	9.5	8.4	67.0	4.7	0.7	9.6	99.9	2.47

The majority of C₃A phases were identified on the diffraction patterns: C₃A cubic (ICSD 00-038-1429), C₃A orthorhombic (ICSD 1880), and C₃A monoclinic (ICSD 100221). The mineral mayenite (ICSD 00-009-0413), lime (ICSD 00-043-1001), and portlandite (ICSD 00-004-0733) as minor phases were also identified.

Figure 3 graphically shows the effect of Na doses on the change in the C₃A polymorphism. The presence of higher Na content is a basic prerequisite for the formation of non-cubic C₃A phases. It can be seen in Table 2 and Figure 3 that at least 2.5–3% Na is needed for the formation of non-cubic phases of tricalcium aluminate. At Na content of 3 to 4%, the formation of the orthorhombic C₃A is supported. At higher doses of Na above 3.5–4%, the monoclinic phase C₃A is formed.

**Figure 3.** Graphical representation of individual mineral contents at different Na contents.

The presence of portlandite is caused by the very rapid hydration of lime due to air moisture. The reason for the higher content of lime, i.e., portlandite, can be determined according to another study [31], with the release of free lime during the formation of a solid solution of C₃A with sodium ions calculated according to the following equation:



The synthesized cubic, Na-substituted orthorhombic, and monoclinic C_3A s were evaluated as mixtures, indicating that accurate quantification is very difficult to perform.

Identification and quantification of cubic C_3A is generally easy because the diffraction lines are well defined and clearly match the reference pattern. Substitution of Na, however, causes significant difficulties because the pattern of cubic and orthorhombic or monoclinic forms significantly overlaps, see Figure 4. Therefore, it is quite difficult to clearly and accurately fit the individual diffraction lines of cubic, orthorhombic, and monoclinic C_3A using the XRD technique.

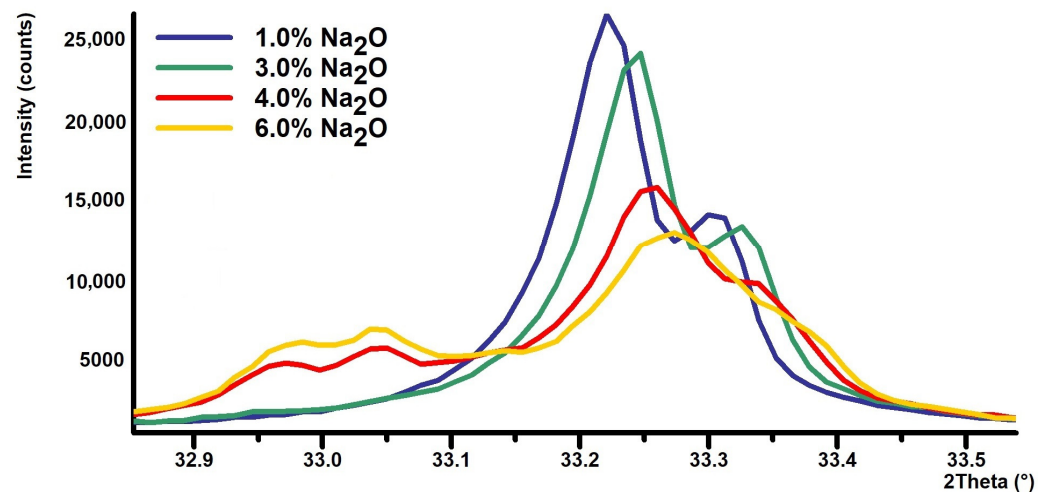


Figure 4. Portion of XRD powder patterns: 1.0% Na_2O (cubic C_3A), 3.0% Na_2O (cubic + orthorhombic C_3A), 4% Na_2O (cubic + orthorhombic + monoclinic C_3A), and 4% Na_2O (mainly monoclinic C_3A).

Unit Cell Volume

The Rietveld method was also used in studying the crystal structure to provide more detailed information about the crystal lattice of the individual polymorph phases of tricalcium aluminate. Table 3 shows the unit cell volumes determined using the Rietveld method, graphically in Figure 5.

Table 3. Unit cell volume of cubic, orthorhombic, and monoclinic C_3A .

Na_2O [%]	Volume [\AA^3]	Volume [\AA^3]	Volume [\AA^3]
0.0	3551.29	0.00	0.00
0.5	3549.51	0.00	0.00
1.0	3546.20	0.00	0.00
1.5	3542.38	0.00	0.00
2.0	3541.13	0.00	0.00
2.5	3540.49	0.00	0.00
3.0	3539.06	1778.56	0.00
3.5	3539.69	1779.86	0.00
4.0	3539.58	1786.13	1780.42
4.5	3541.50	1785.70	1779.76
5.0	3540.52	1787.93	1779.63
5.5	3537.95	1786.49	1782.00
6.0	3537.86	1786.68	1788.58

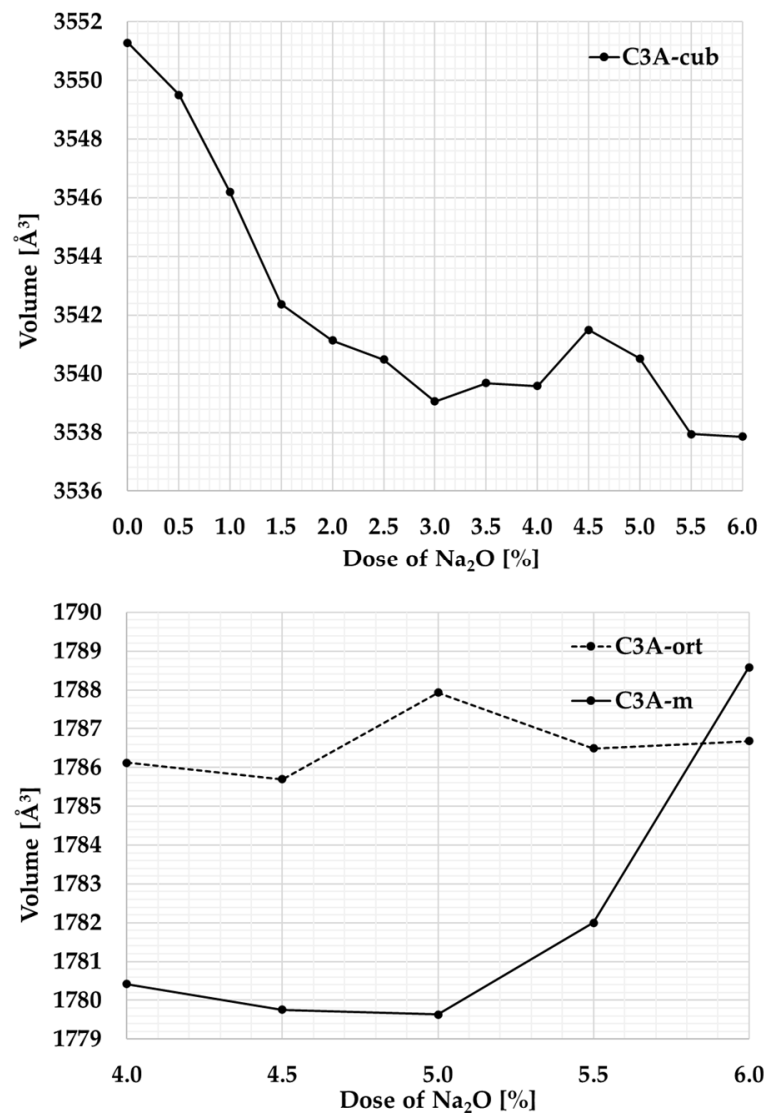


Figure 5. Graphical representation of changes in the unit cell volume at different Na contents.

Sodium (Na), which replaces calcium (Ca) in the crystal lattice, occupies a space that is slightly larger. When sodium is replaced by calcium, the spaces between the atoms are not filled, leading to a gradual change in the crystal structure. As a result, the initially symmetric cubic lattice becomes a less symmetric orthorhombic and subsequently monoclinic structure. At Na content of 3%, the mixture contains cubic C₃A with a unit cell volume of around 3545 Å³ and orthorhombic C₃A with almost half the volume of the unit cell.

3.3. Tricalcium Aluminate Crystallinity

To supplement more detailed information and connections with the origin and development of the C₃A polymorphism, the development of crystallinity was monitored.

The size of the crystallites was evaluated in the normal to appropriate crystallographic plane that had the main crystallographic direction and was sufficiently intense. A distinct crystallographic plane determined by the Miller indices “hkl”: 004 was chosen, which appears on the diffraction pattern at the position 2θ : 33.177°; see Figure 6.

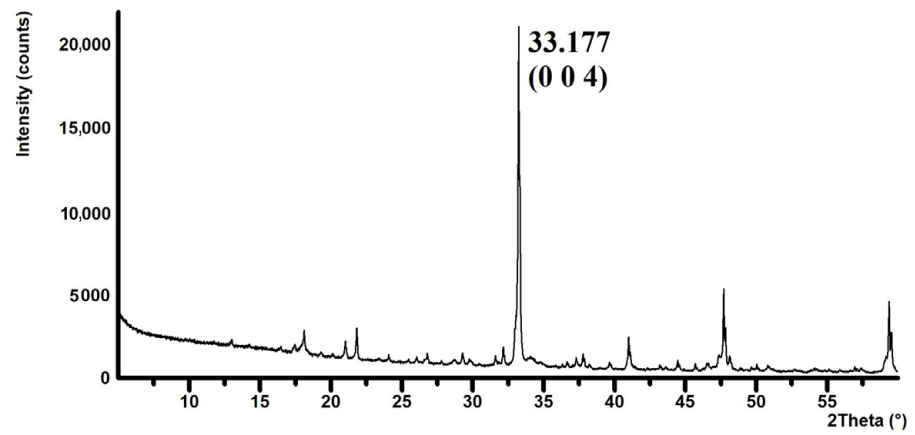


Figure 6. Details of the reflection of the selected crystallographic plane (0 0 4) on the XRD pattern.

The Sherrer method was used to calculate the crystallite size. Table 4 and Figure 7 graphically show the crystallite sizes for individual samples.

Table 4. Crystallite size of cubic, orthorhombic, and monoclinic C₃A (L Vol-FWHM).

Na ₂ O [%]	L [Å]	L [Å]	L [Å]
0.0	1233.6	0.0	0.0
0.5	1184.3	0.0	0.0
1.0	1264.8	0.0	0.0
1.5	1233.6	0.0	0.0
2.0	1249.0	0.0	0.0
2.5	1208.4	0.0	0.0
3.0	C ₃ A-cub 1320.5	C ₃ A-ort 332.7	C ₃ A-m 0.0
3.5	1320.5	466.2	0.0
4.0	1320.5	602.2	680.0
4.5	659.3	467.9	1320.5
5.0	457.2	580.5	1047.8
5.5	455.6	711.2	1262.5
6.0	467.4	467.4	1212.5

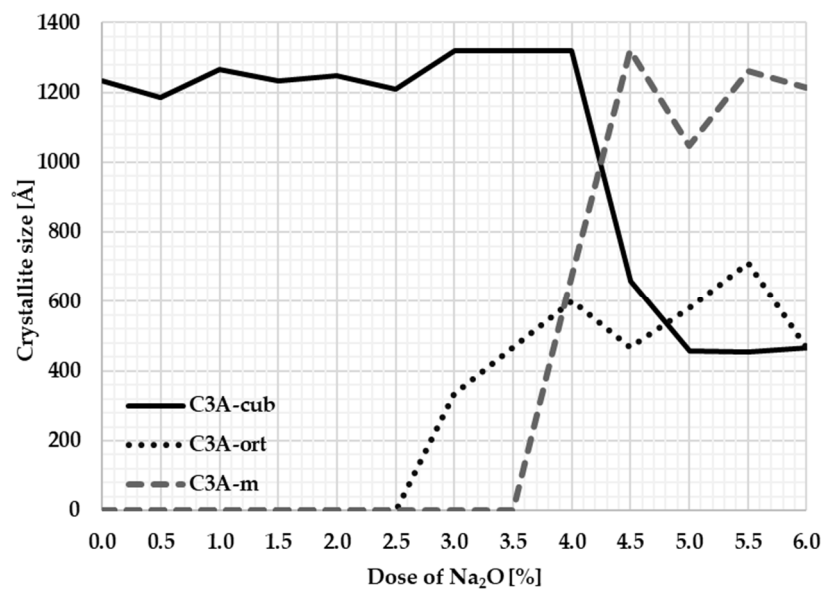


Figure 7. Dependence of crystallite size on Na content.

The course of the crystallite size corresponds to the changes in the unit cell during the transformations of the individual crystal structures. Based on the calculation of the size of the crystallites, it can be stated that the most significant changes in crystallinity occur at Na₂O content of between 3 and 4 percent when there is a fundamental polymorphic change from cubic to orthorhombic. The average crystallite size of cubic C₃A is around 1200 Å. When the sodium ions are incorporated into the C₃A cubic structure, the size of its crystallites rapidly decreases to an average value of 466 Å. At 4% sodium content, the orthorhombic structure changes to a monoclinic structure. The average crystallite size of the monoclinic structure is around 1104 Å and approaches the crystallite size of the original cubic C₃A.

4. Conclusions

The results obtained in this study allow the following conclusions to be reached:

- The various polymorphs of C₃A were prepared through the method of solid-state synthesis and a procedure close to the real conditions of the formation of Portland clinker.
- The presence of multiple polymorphs might be due to the particle size of the raw meal.
- Although powder diffraction has a fundamental limitation in the reliable identification and quantification of C₃A polymorphs, it is the only accessible approach.
- The stability of cubic tricalcium aluminate is up to 2.5% Na content.
- The formation of orthorhombic tricalcium aluminate using solid-state synthesis, as described, requires Na content of at least 3–3.5% Na.
- The transition from an orthorhombic structure to a monoclinic structure takes place at 4–4.5% Na content.
- The most significant changes in crystallinity occur at 3–4% Na content.
- There are no clearly defined boundaries for the existence of individual C₃A phases, these phases arise at the same time and overlap each other in the areas of their formation at different Na doses.

Author Contributions: Conceptualization, S.R. and K.D.; methodology, S.R.; software, K.D. and D.V.; validation, S.R., K.D. and A.J.; formal analysis, M.B.; investigation, S.R. and K.D.; resources, S.R.; data curation, K.D.; writing—original draft preparation, S.R.; writing—review and editing, S.R. and K.D.; visualization, S.R.; supervision, K.D. and S.R.; project administration, S.R.; K.D. and M.B.; funding acquisition, K.D. and S.R. All authors have read and agreed to the published version of the manuscript.

Funding: We acknowledge the financial support given to the project “Study of the formation and stability of various tricalcium aluminate polymorphs” (FAST-S-23-8246) and the project of the Czech Science Foundation “The role combination of fluxes and mineralizers on properties of low-energy clinker” (23-05122S).

Institutional Review Board Statement: Not applicable.

Informed Consent Statement: Not applicable.

Data Availability Statement: Data are contained within the article.

Conflicts of Interest: The authors declare no conflicts of interest.

Appendix A

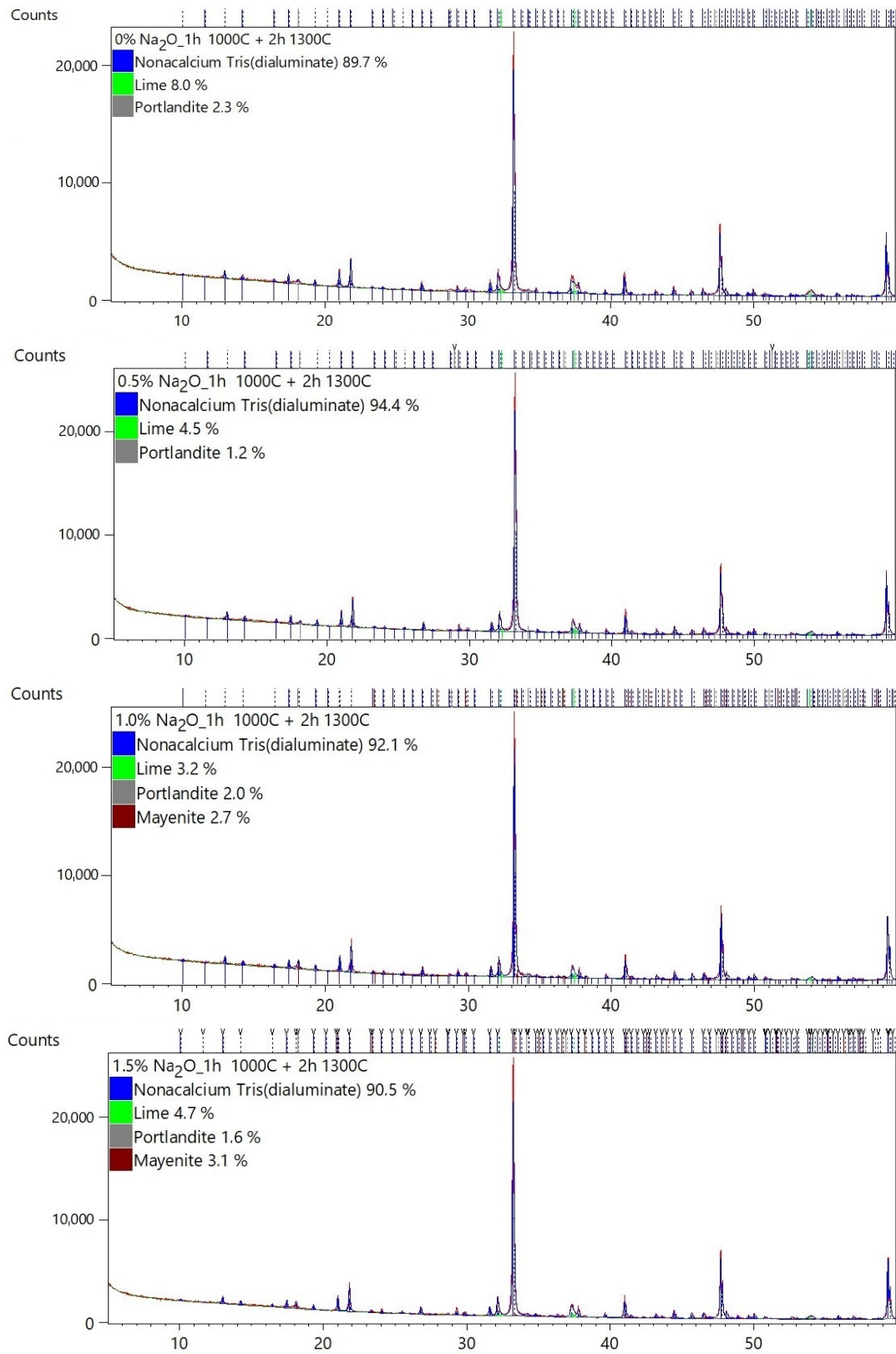


Figure A1. Cont.

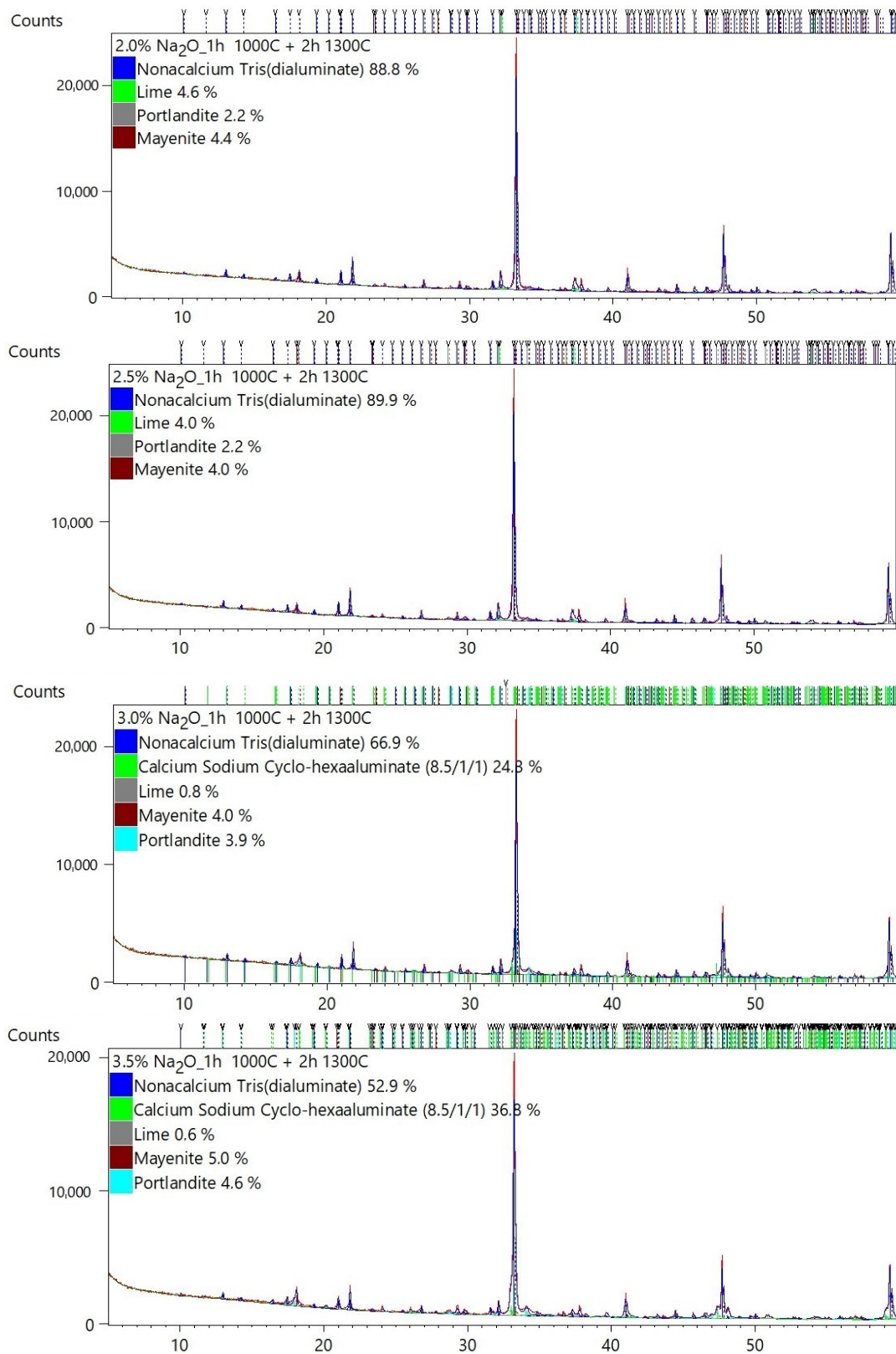


Figure A1. Cont.

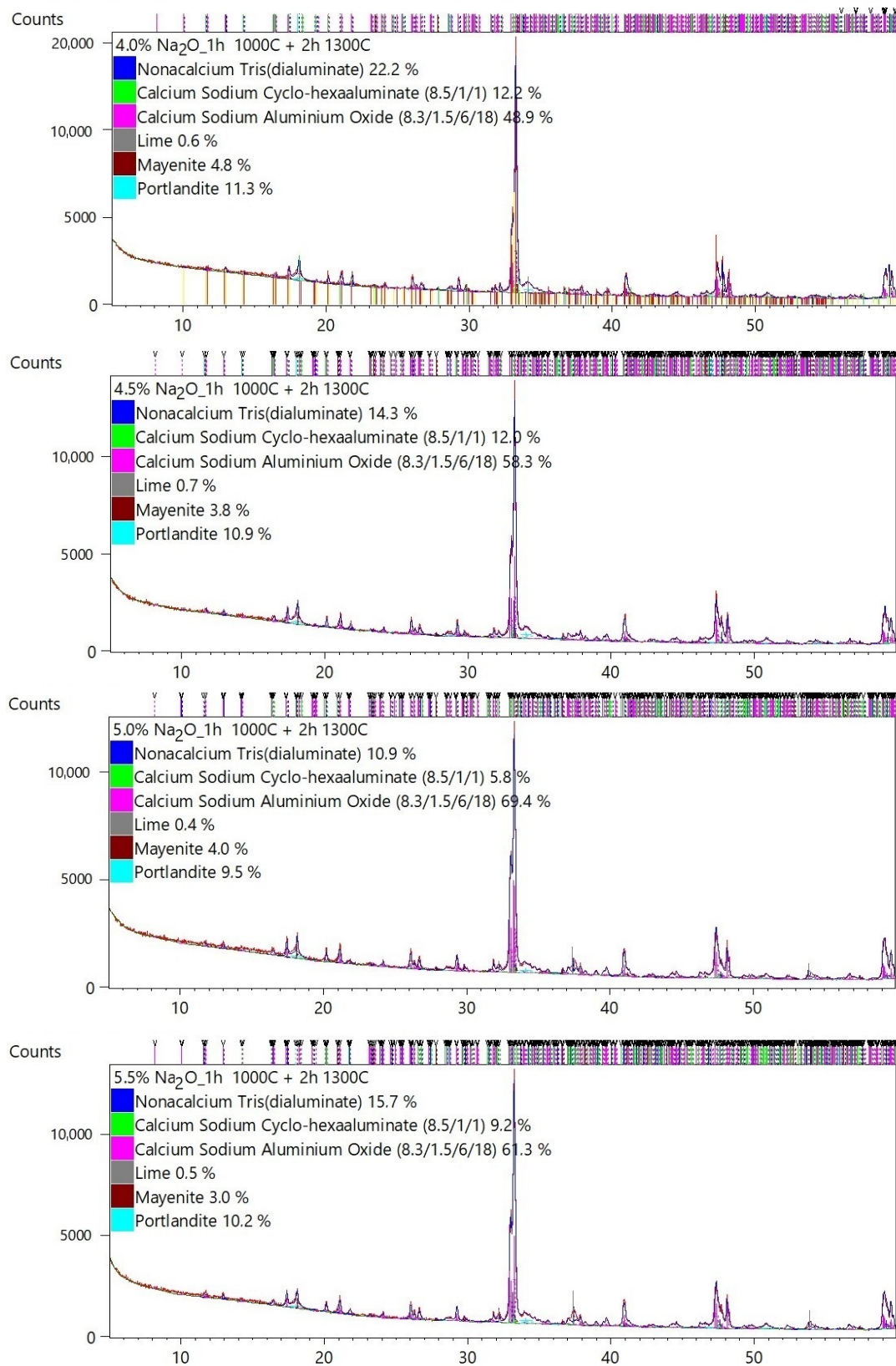


Figure A1. Cont.

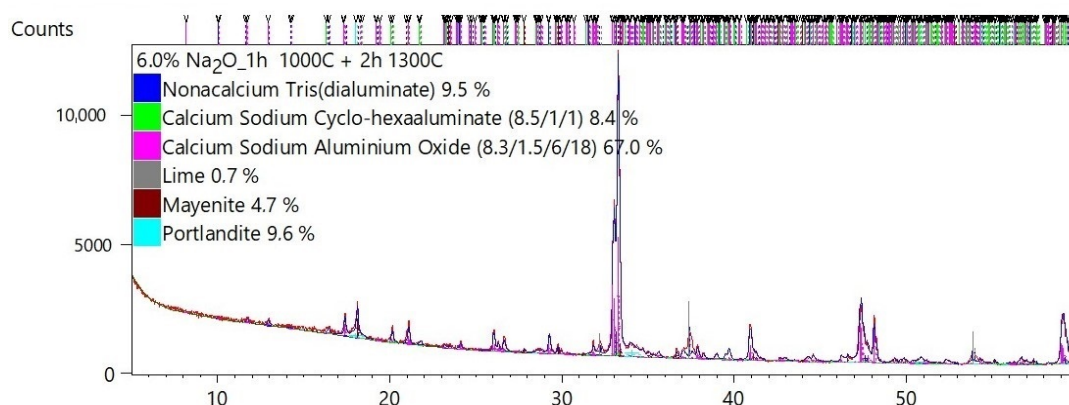


Figure A1. Rietveld analysis results.

References

- Scrivener, K.L.; John, V.M.; Gartner, E.M. Eco-efficient cements: Potential economically viable solutions for a low-CO₂ cement-based materials industry. *Cem. Concr. Res.* **2018**, *114*, 2–26. [CrossRef]
- CEMBUREAU, 2050 Carbon Neutrality Roadmap. Available online: <https://cembureau.eu/library/reports/2050-carbon-neutrality-roadmap/> (accessed on 29 November 2023).
- Schneider, M.; Hoenic, V.; Ruppert, J.; Rickert, J. The cement plant of tomorrow. *Cem. Concr. Res.* **2023**, *173*, 107290. [CrossRef]
- CEMBUREAU, Energy Assessment for CCUS Options EU Cement Sector. Available online: <https://cembureau.eu/media/bucbkisd/230503-tno-r10586-1-energy-assessment-for-ccus-options-eu-cement-sector-final.pdf> (accessed on 29 November 2023).
- Szabó, L.; Hidalgo, I.; Císcar, J.C.; Soria, A.; Russ, P. *Energy Consumption and CO₂ Emissions from the World Cement Industry*; European Commission Joint Research Center: Brussels, Belgium, 2003.
- Mokrzycki, E.; Uliasz-Bocheńczyk, A. Alternative fuels for the cement industry. *Appl. Energy* **2003**, *74*, 95–100. [CrossRef]
- Taylor, H.F.W. *Cement Chemistry*; Academic Press: London, UK, 1990.
- Hewlett, P.C. *Leas 's Chemistry of Cement and Concrete*; Arnold: London, UK, 1998; pp. 131–193.
- Wesselsky, A.; Jensen, O.M. Synthesis of pure Portland cement phases. *Cem. Concr. Res.* **2009**, *39*, 973–980. [CrossRef]
- Rodríguez, N.H.; Martínez-Ramírez, S.; Blanco-Varela, M.T.; Donatello, S.; Guillem, M.; Puig, J.; Fos, C.; Larrotcha, E.; Flores, J. The effect of using thermally dried sewage sludge as an alternative fuel on Portland cement clinker production. *J. Clean. Prod.* **2013**, *52*, 94–102. [CrossRef]
- Nakomcic-Smaragdakis, B.; Cepic, Z.; Senk, N.; Doric, J.; Radovanovic, L. Use of scrap tires in cement production and their impact on nitrogen and sulfur oxides emissions. *Energy Sources* **2016**, *38*, 485–493. [CrossRef]
- Tsilivianis, C.A. Alternative fuels in cement manufacturing: Modeling for process optimization under direct and compound operation. *Fuel* **2012**, *99*, 20–39. [CrossRef]
- Bingrong, L.; Wei, Y.; Peng, C.; Zhou, H.; Li, S.; Wang, S. Influence of Fe₂O₃ on the hydration kinetics of tricalcium aluminate. *J. Eur. Ceram. Soc.* **2023**, *43*, 6550–6561.
- Chen, S.; Chen, G.; Cheng, J. Effect of additives on the hydration resistance of materials synthesized from the magnesia-calcia system. *J. Am. Ceram. Soc.* **2000**, *88*, 1810–1812. [CrossRef]
- Tian, Y.; Pan, X.; Yu, H.; Tu, G. Formation mechanism and crystal simulation of Na₂O-doped calcium aluminate compounds. *Trans. Nonferrous Met. Soc. China* **2016**, *26*, 849–858. [CrossRef]
- Boikova, A.I.; Domanskii, A.I.; Paramonova, V.A.; Stavitskaya, G.P.; Nikushchenko, V.M. The influence of sodium oxide on the structure and properties of tricalcium aluminate. *Cem. Concr. Res.* **1977**, *7*, 483–491. [CrossRef]
- Mondal, P.; Jeffrey, J.W. Crystal structure of tricalcium aluminate, Ca₃Al₂O₆. *Acta Crystallogr.* **1975**, *31*, 689–697. [CrossRef]
- Nguyen, M.; Sokolář, R. Formation and influence of magnesium-alumina spinel on the properties of refractory forsterite-spinel ceramics. *Mater. Technol.* **2020**, *54*, 135–141. [CrossRef]
- Gobbo, L.; Sant'Agostino, L.; Garcez, L. C₃A polymorphs related to industrial clinker alkalis content. *Cem. Concr. Res.* **2004**, *34*, 657–664. [CrossRef]
- Dietmar, S.; Wistuba, S. Crystal structure refinement and hydration behaviour of doped tricalcium aluminate. *Cem. Concr. Res.* **2006**, *36*, 2011–2020.
- Nishi, F.; Takeuchi, Y. Aluminum oxide (Al₆O₁₈) rings of tetrahedra in the structure of sodium calcium aluminate (Ca_{8.5}NaAl₆O₁₈). *Acta Crystallogr.* **1975**, *31*, 1169–1173. [CrossRef]
- Götz-Neunhoffer, F.; Neubauer, J. Crystal structure refinement of Na-substituted C₃A by Rietveld analysis and quantification in OPC. In Proceedings of the 10th International Congress on the Chemistry of Cement, Gothenburg, Sweden, 2–6 June 1997.
- Varma, S.P.; Wall, C.D. A monoclinic tricalcium aluminate (C₃A) phase in a commercial Portland cement clinker. *Cem. Concr. Res.* **1981**, *11*, 567–574. [CrossRef]
- Singh, V.K.; Ali, M.M.; Mandal, U.K. Formation Kinetics of Calcium Aluminates. *J. Am. Ceram. Soc.* **1990**, *73*, 872–876. [CrossRef]

25. Mohamed, B.M.; Sharp, J.H. Kinetics and mechanism of formation of tricalcium aluminate, $\text{Ca}_3\text{Al}_2\text{O}_6$. *Thermochim. Acta* **2002**, *388*, 105–114. [[CrossRef](#)]
26. López, F.A.; Martín, M.I.; Alguacil, F.J.; Sergio Ramírez, M.; González, J.R. Synthesis of Calcium Aluminates from Non-Saline Aluminum Dross. *Materials* **2019**, *12*, 1837. [[CrossRef](#)] [[PubMed](#)]
27. Pati, R.K.; Panda, A.B.; Pramanik, P. Preparation of Nanocrystalline Calcium Aluminate Powders. *J. Mater. Synth. Process.* **2002**, *10*, 157–161. [[CrossRef](#)]
28. Mandić, V.; Kurajica, S. The influence of solvents on sol–gel derived calcium aluminate. *Mater. Sci. Semicond. Process.* **2015**, *38*, 306–313. [[CrossRef](#)]
29. Ghoroi, C.; Suresh, A.K. Solid–solid reaction kinetics: Formation of tricalcium aluminate. *AIChE J.* **2007**, *53*, 502–513. [[CrossRef](#)]
30. Shin, G.Y.; Glasser, F.P. Interdependence of sodium and potassium substitution on tricalcium aluminate. *Cem. Concr. Res.* **1982**, *13*, 135–170. [[CrossRef](#)]
31. Ostrowski, C.; Želazny, J. Solid Solutions of Calcium Aluminates C3A, C12A7 and CA with Sodium Oxide. *J. Therm. Anal. Calorim.* **2004**, *75*, 867–885. [[CrossRef](#)]
32. Scherrer, P. Bestimmung der Grosse und der Inneren Struktur von Kolloidteilchen Mittels Rontgenstrahlen. *Nachrichten Von Der Ges. Der Wiss. Math.-Phys. Kl.* **1918**, *2*, 98–100.
33. Warren, B.E. *X-ray Diffraction*; Addison-Wesley: Boston, MA, USA, 1969.
34. Ravaszová, S.; Dvořák, K. Development of Crystallinity of Triclinic Polymorph of Tricalcium Silicate. *Materials* **2020**, *13*, 3734. [[CrossRef](#)]

Disclaimer/Publisher’s Note: The statements, opinions and data contained in all publications are solely those of the individual author(s) and contributor(s) and not of MDPI and/or the editor(s). MDPI and/or the editor(s) disclaim responsibility for any injury to people or property resulting from any ideas, methods, instructions or products referred to in the content.